

Order parameter of superfluid $^3\text{He-B}$ near surfaces

Weiye Zhang and J. Kurkijärvi

Department of Technical Physics, Helsinki University of Technology, Rakentajanaukio 2 C, 02150 Espoo, Finland

E. V. Thuneberg

Research Institute for Theoretical Physics, University of Helsinki, Siltavuorenpenger 20 C, 00170 Helsinki, Finland

(Received 5 February 1987)

The order parameter of superfluid $^3\text{He-B}$ is calculated near surfaces with the quasiclassical theory and a thin-dirty-layer surface-scattering model. The surface structures depend on the temperature, the surface roughness, the Fermi-liquid parameters, and the mass superflow tangential to the surface. All these are studied with special emphasis on the roughness and the superflow. A numerical technique of solving the quasiclassical equations is discussed.

I. INTRODUCTION

The superfluid state at the surface of an ordinary s -wave superconductor is essentially the same as that in the bulk, if the effects of a magnetic field are not considered. In p -wave superfluids—such as ^3He and conceivably some heavy-fermion superconductors—this is not the case. There the order parameter is weakened within a couple of coherence lengths ($\xi_0 \approx 15$ nm) from a wall by quasiparticle scattering at the surface. The different spatial components of the order parameter are handled unequally and the structure of the order parameter becomes complicated and sensitive to the scattering properties of the wall. We study the equilibrium surface structure of the order parameter in the B phase of superfluid ^3He .

The surface structure of the order parameter is of interest for several reasons. A surface imposes a boundary condition on the hydrodynamics of the bulk.¹ An example is the hydrodynamic theories of the normal and superfluid components of a superfluid. The classical boundary condition for the normal fluid is the vanishing of the velocity at a stationary wall. In low-temperature Fermi systems, the mean free path of quasiparticles may become very long, rendering the classical condition inadequate. A simple remedy is a “slip boundary condition” which requires the extrapolation of the tangential velocity to vanish at a slip length ζ behind the wall.² The order parameter at the surface influences the scattering of quasiparticles (Andreev reflection) and thus enters into the theoretical calculation of the slip length.³ For the superfluid fraction, a surface imposes boundary conditions on the texture of the order parameter, the direction of the \hat{n} vector in the B phase⁴ and the direction of the \hat{l} vector in the A phase.⁵ In some cases boundary conditions can be deduced from symmetries alone. In general, they depend on the tangential superfluid velocity and the magnetic field and have to be determined from the exact configuration of the order parameter. At high superfluid velocities there are the great unsolved problems of vortex nucleation and critical velocities. The determination of the equilibrium surface order parameter is a first step towards their resolution. There is also a recent theoretical result by Thuneberg⁶ that the conventional surface struc-

ture of the B phase,⁴ under certain conditions, may spontaneously break its symmetry and form an A -phase-like structure at the wall. On the experimental side, there are several recent observations of dissipation or critical velocities^{7–10} that may be directly related to surfaces. Finally, surface structures may be important in identifying heavy-fermion superconductors such as CeCu_2Si_2 , UPt_3 , UBe_{13} , etc. The tunneling spectra are expected to be different in p -wave superconductors from those in ordinary s -wave superconductors. They are clearly related to surface states.

In the present work, surface structures at rough walls are calculated with the quasiclassical theory of ^3He .¹¹ The scattering of quasiparticles off rough surfaces is treated in terms of a one-parameter model by Culetto *et al.*¹² Surface structures have been studied previously in the case of specular surface scattering¹³ and also for the rough surface with a more complicated boundary condition than here.¹⁴ The most important limitation of the present analysis is the restriction of the weak-coupling version of the quasiclassical theory. Although we can reach temperatures lower than the Ginzburg-Landau region we can see no explicit strong-coupling effects, such as the anomalous surface state of Ref. 6. On the other hand, we do take into account the Fermi-liquid corrections. In practice, this seems to mean including the most important, F_1^s , which couples to the supercurrent. The inclusion of further parameters would be straightforward.

We have computed the order parameter for varying degrees of roughness (defined below) and temperatures in the absence of a current. The effect of a current was also investigated, i.e., a constant phase gradient was imposed along a specular surface. This was done at the reduced temperature $T/T_c = t = 0.8$ at which the phase transition curve of Pekola *et al.*⁸ takes its minimum pressure (< 15 bars). Three values of the Landau parameter F_1^s were assumed, $F_1^s = 0, 9.27$ (9 bars pressure) (Ref. 15) and 13.18 (24 bars pressure). Finally, the combined effect of the surface roughness and the current was studied at $t = 0.8$, $F_1^s = 9.27$. Nowhere did we observe a change in the symmetry of the order parameter. All our results have the symmetries P_1, P_2, P_3 , as discussed in Sec. IV.

Nevertheless, we did observe a metastable state separate from the one that continuously arises out of what we be-

lieve to be the state of lowest energy (“regular” state) in the absence of current. In the metastable state the real part of the order-parameter component parallel to the current goes to zero at the surface. Strangely enough, this state, as does the strong-coupling state of Ref. 6, remains metastable in the limit of vanishing current.

The surface structures have the curious property that even the simplest state without mass current has macroscopic spin currents flowing along the surface. Such currents are consistent with the rotational symmetry around the surface normal $\hat{\mathbf{x}}$ because spins pointing in the $\hat{\mathbf{s}}$ direction flow in the direction $\hat{\mathbf{s}} \times \hat{\mathbf{x}}$. This may favor the nucleation of spin-current vortices.¹⁶

We also discuss the numerical solution of the quasiclassical equation. The equations can be reduced to a first-order differential equation for a five-component complex vector in the absence of magnetic field irrespective of the form of the order parameter. In the present paper, nevertheless, we used a ten-component vector representation and apply the multiplication trick only outside the scattering layer.

The rest of the paper is organized as follows. In Sec. II, we discuss some general aspects of the quasiclassical theory as they apply to the present problem. In Sec. III we discuss on surface models and boundary conditions and in Sec. IV a symmetry classification of the surface states. In Sec. V we analyze the quasiclassical equation in some detail and discuss the technical aspects of its numerical treatment. Our results are presented in Sec. VI and their implications are discussed. A preliminary report of a part of the present results has appeared elsewhere.¹⁷

II. BULK QUASICLASSICAL THEORY

The quasiclassical theory of Fermi systems describes slowly varying phenomena in space and time. Characteristic lengths have to be large on the scale of the Fermi wavelength k_F^{-1} and characteristic times long on the scale of the inverse Fermi frequency $\hbar E_F^{-1}$. Superfluid phenomena belong to the required category with a large margin with $\Delta \ll E_F$ and $\xi_0 = \hbar v_F / 2\pi k_B T_c \gg k_F^{-1}$. The quasiclassical theory covers all the hydrodynamic effects such as transport of mass, heat, momentum, and spin as well as nonhydrodynamic collective modes and the complete thermodynamics of a superfluid. Because the quasiclassical theory eliminates a great deal of fine structure right at the outset, it is well suited for numerical calculation. The input information of the quasiclassical weak-coupling scheme is the superfluid transition temperature and Landau Fermi-liquid parameters (including the Fermi velocity). The strong-coupling version needs the full scattering amplitude of a pair of quasiparticles at the Fermi surface in addition to the above. A review of the quasiclassical theory can be found in Ref. 11.

The state of liquid ^3He is represented by a quasiclassical propagator \hat{g} which is a 4×4 single-particle matrix Green's function integrated over the magnitude of the momentum. The Matsubara propagator satisfies the transportlike or the Eilenberger-Larkin-Ovchinnikov-Eliashberg (ELOE) equation:¹¹

$$[i\varepsilon_n \hat{\tau}_3 - \hat{\sigma}(\hat{\mathbf{k}}, \mathbf{R}; \varepsilon_n), \hat{g}(\hat{\mathbf{k}}, \mathbf{R}; \varepsilon_n)] + i\hbar v_F \hat{\mathbf{k}} \cdot \nabla \hat{g}(\hat{\mathbf{k}}, \mathbf{R}; \varepsilon_n) = 0, \quad (1a)$$

$$[\hat{g}(\hat{\mathbf{k}}, \mathbf{R}; \varepsilon_n)] = -(\pi\hbar)^2. \quad (1b)$$

The ELOE equation is an ordinary first-order differential equation along “trajectories,” lines parallel to $\hat{\mathbf{k}}$, and Eq. (1b) is a normalization condition. Here, $[\hat{A}, \hat{B}] = \hat{A}\hat{B} - \hat{B}\hat{A}$ and ε_n is the Matsubara frequency, $\varepsilon_n = \pi k_B T(2n+1)$. A caret denotes (either the unit vector $\hat{\mathbf{k}}$ or) a 4×4 matrix, which is a product of the spin space and the Nambu particle-hole space. The Pauli matrices in these two spaces are denoted by σ_i and $\hat{\tau}_i$, respectively. The self-energy is parametrized as

$$\hat{\sigma}(\hat{\mathbf{k}}, \mathbf{R}; \varepsilon_n) = \begin{bmatrix} v + \mathbf{v} \cdot \boldsymbol{\sigma} & \Delta \cdot \boldsymbol{\sigma} i \sigma_2 \\ i \sigma_2 \Delta^* \cdot \boldsymbol{\sigma} & \underline{v} - \sigma_2 \underline{\mathbf{v}} \cdot \boldsymbol{\sigma} \sigma_2 \end{bmatrix}, \quad (2a)$$

and the Green's function as

$$\hat{g}(\hat{\mathbf{k}}, \mathbf{R}; \varepsilon_n) = \begin{bmatrix} g + \mathbf{g} \cdot \boldsymbol{\sigma} & (f + \mathbf{f} \cdot \boldsymbol{\sigma}) i \sigma_2 \\ i \sigma_2 (f + \mathbf{f} \cdot \boldsymbol{\sigma}) & \underline{g} - \sigma_2 \underline{\mathbf{g}} \cdot \boldsymbol{\sigma} \sigma_2 \end{bmatrix}. \quad (2b)$$

The self-consistency equations

$$\mathbf{v}(\hat{\mathbf{k}}, \mathbf{R}) = \frac{k_B T}{\hbar} \sum_n \int \frac{d\Omega'}{4\pi} A^s(\hat{\mathbf{k}} \cdot \hat{\mathbf{k}}') \mathbf{g}(\hat{\mathbf{k}}', \mathbf{R}; \varepsilon_n), \quad (3a)$$

$$\mathbf{v}(\hat{\mathbf{k}}, \mathbf{R}) = \frac{k_B T}{\hbar} \sum_n \int \frac{d\Omega'}{4\pi} A^a(\hat{\mathbf{k}} \cdot \hat{\mathbf{k}}') \mathbf{g}(\hat{\mathbf{k}}', \mathbf{R}; \varepsilon_n), \quad (3b)$$

$$\frac{k_B T}{\hbar} \sum_n \left[\int \frac{d\Omega'}{4\pi} 3(\hat{\mathbf{k}} \cdot \hat{\mathbf{k}}') \mathbf{f}(\hat{\mathbf{k}}', \mathbf{R}; \varepsilon_n) - \frac{\pi \hbar \Delta(\hat{\mathbf{k}}, \mathbf{R})}{[\varepsilon_n^2 + \Delta^2(T)]^{1/2}} \right] = 0 \quad (3c)$$

determine the self-energy in (1). The functions A in the first two can be represented as

$$A^{s,a}(\hat{\mathbf{k}} \cdot \hat{\mathbf{k}}') = \sum_l \frac{F_l^{s,a}}{1 + F_l^{s,a}/(2l+1)} P_l(\hat{\mathbf{k}} \cdot \hat{\mathbf{k}}'),$$

where $F_l^{s,a}$ are the Landau Fermi-liquid parameters. The gap equation (3c) is written in a cutoff-independent form by introducing $\Delta(T)$, the (temperature-dependent) gap in the bulk liquid. In the absence of boundaries the equations above are a closed set which allows the computation of the Green's function and the self-energies. Out of these one can deduce the physical quantities. For example, the mass current and the spin current are given by

$$\mathbf{J}(\mathbf{R}) = \frac{2v_F k_B T}{\hbar} \sum_n \int \frac{d\Omega}{4\pi} N(E_F) \hat{\mathbf{k}} \mathbf{g}(\hat{\mathbf{k}}, \mathbf{R}; \varepsilon_n), \quad (4a)$$

$$\mathbf{J}(\mathbf{R})_{\alpha,i} = v_F k_B T \sum_n \int \frac{d\Omega}{4\pi} N(E_F) k_i \mathbf{g}_\alpha(\hat{\mathbf{k}}, \mathbf{R}; \varepsilon_n). \quad (4b)$$

The Matsubara propagators and the self-energies satisfy the basic symmetry relations

$$\{[\hat{u}(\hat{\mathbf{k}}, \mathbf{R}; \varepsilon_n)]^{\text{tr}}\}^* = \hat{\tau}_3 \hat{u}(\hat{\mathbf{k}}, \mathbf{R}; -\varepsilon_n) \hat{\tau}_3, \quad (5a)$$

$$[\hat{u}(\hat{\mathbf{k}}, \mathbf{R}; \varepsilon_n)]^{\text{tr}} = \hat{\tau}_2 \hat{u}(-\hat{\mathbf{k}}, \mathbf{R}; -\varepsilon_n) \hat{\tau}_2, \quad (5b)$$

where \hat{u} stands either for \hat{g} or $\hat{\sigma}$ and tr denotes the transpose matrix. Hence only a calculation at positive energies and in one half-space of the directions of the trajectories is required. The symmetries (5) follow directly from the definition of the propagators. In addition, Eq. (1) has the symmetry

$$[\hat{u}(\hat{\mathbf{k}}, \mathbf{R}; \varepsilon_n)]^{\text{tr}} = -\hat{\tau}_2 \hat{u}(\hat{\mathbf{k}}, \mathbf{R}; \varepsilon_n) \hat{\tau}_2. \quad (6)$$

This symmetry applies in the absence of a magnetic field in the ELOE equation (1) (because the gap has definite parity). It follows from this symmetry that the solution of (1) has no magnetic moment on the order of $\mu_N N(E_F) \Delta$, i.e., the magnetic moment given by an equation of the type (4) is zero. However, symmetry (6) is not the time-inversion symmetry: it does not constrain the form of the order parameter and it does not exclude a magnetic moment on the order of $\mu_N N(E_F) \Delta^2 / E_F$ arising from a violation of the particle-hole symmetry. Near the transition temperature the magnetization is given by¹⁸

$$\mathbf{M}(\mathbf{R}) = iC \int \frac{d\Omega}{4\pi} \Delta(\hat{\mathbf{k}}, \mathbf{R}) \times \Delta^*(\hat{\mathbf{k}}, \mathbf{R}), \quad (7)$$

where $C \sim N'(E_F)$. This is nonzero for surface states at zero field in general. Unfortunately, its reliable theoretical evaluation at a general temperature is not simple: In order to be consistent, one has to take into account the particle-hole asymmetry in both the density of states and in the pairing interaction, and there is no exact relation connecting the two. Their relative contributions vary as functions of the temperature, i.e., at least two phenomenological parameters are needed.

III. BOUNDARY CONDITION

At surfaces the quasiclassical equations (1) have to be supplemented with boundary conditions. A fully general boundary condition within the quasiclassical theory of superfluidity was first derived by Buchholtz and Rainer.¹⁹ This condition requires a surface scattering t matrix for quasiparticles at the Fermi energy and turns out to be too cumbersome for practical calculations. It is more convenient to take advantage of models imitating surfaces. The simplest such model is the specular surface, where the quasiparticle momentum along the surface is conserved. In terms of the quasiparticle propagator this condition takes the form

$$\hat{g}(\hat{\mathbf{k}}, \mathbf{R}_{\text{surf}}; \varepsilon_n) = \hat{g}(\hat{\mathbf{k}} - 2\hat{\mathbf{x}}(\hat{\mathbf{k}} \cdot \hat{\mathbf{x}}), \mathbf{R}_{\text{surf}}; \varepsilon_n), \quad (8)$$

where $\hat{\mathbf{x}}$ is the unit vector normal to the wall and \mathbf{R}_{surf}

$$p = \frac{2}{\pi} \int d\Omega_{\text{in}} \int d\Omega_{\text{out}} |\hat{\mathbf{x}} \cdot \hat{\mathbf{k}}_{\text{in}}| \frac{dp}{d\Omega_{\text{out}}}(\hat{\mathbf{k}}_{\text{out}}, \hat{\mathbf{k}}_{\text{in}})(\hat{\mathbf{x}} \times \hat{\mathbf{k}}_{\text{in}}) \cdot [\hat{\mathbf{x}} \times (\hat{\mathbf{k}}_{\text{in}} - \hat{\mathbf{k}}_{\text{out}})], \quad (11)$$

where $(dp/d\Omega_{\text{out}})(\hat{\mathbf{k}}_{\text{out}}, \hat{\mathbf{k}}_{\text{in}})$ is the differential scattering probability from the momentum direction $\hat{\mathbf{k}}_{\text{in}}$ to the direction $\hat{\mathbf{k}}_{\text{out}}$. The value $p=0$ corresponds to specular and $p=1$ to fully diffuse scattering. In the present model, all particles scattered in the impurity layers are counted as

denotes the position on the surface. The order parameter and the density of states near a specular wall have been calculated by Buchholtz and Zwicky.¹³ Obviously, the specular model cannot imitate a rough surface. Buchholtz¹⁴ mimicked the rough wall with the ‘‘random-ripple-wall model’’ where the location of the wall is allowed to fluctuate around a smooth average. This model has two parameters relating to the height of the irregularities and their ‘‘wave vector’’ along the surface.

We chose the boundary condition of Culetto *et al.*¹² who studied the proximity effect in superconductors. Their model consists of a specularly reflecting surface coated with a layer containing impurities. The layer has the thickness d and a scattering mean free path l . Both d and l are imagined as going to zero with their ratio maintained at a constant value. The ratio $\rho = d/l$ then describes the diffusivity of the scattering; with $\rho=0$ the scattering is specular and with $\rho=\infty$ fully diffuse.

The thin-dirty-layer boundary condition can be expressed mathematically as follows. In the scattering layer the Green’s function obeys the same equation as in the bulk, but generalized to take into account the impurity scattering. In the limit of short mean free path, only the impurity-scattering term and the gradient term perpendicular to the surface survive,

$$[\hat{g}(\hat{\mathbf{k}}, \xi, \mathbf{R}_{\text{surf}}; \varepsilon_n), \hat{\sigma}_{\text{imp}}(\xi, \mathbf{R}_{\text{surf}}; \varepsilon_n)] + \frac{2\pi i}{\rho} k_x \frac{d}{d\xi} \hat{g}(\hat{\mathbf{k}}, \xi, \mathbf{R}_{\text{surf}}; \varepsilon_n) = 0, \quad (9)$$

where the impurity self-energy is

$$\hat{\sigma}_{\text{imp}}(\xi, \mathbf{R}_{\text{surf}}; \varepsilon_n) = \int \frac{d\Omega'}{4\pi} \hat{g}(\hat{\mathbf{k}}', \xi, \mathbf{R}_{\text{surf}}; \varepsilon_n). \quad (10)$$

Here the variable ξ denotes the position in the scattering layer; $\xi=0$ corresponds to the specular wall and $\xi=1$ to the interface between the scattering layer and the bulk. On the interface it is natural to require \hat{g} to be continuous; on the specular-wall side the specular reflection boundary condition (8) has to be imposed. The normalization condition (1b) remains valid in the scattering layer.

It must be stressed that this boundary condition is a model. It is therefore not necessary to treat the impurity scattering in higher order than the self-consistent Born approximation or to consider coherent scattering from the infinitely dense impurities. It is only important that the model be a mathematically well-behaved, simple, and intuitive one-parameter boundary condition.

The parameter ρ can be related to other diffusivity parameters in the literature. Lüders and Usadel define²⁰ their diffusivity parameter p as

diffusively scattered. It is simple to deduce from Eq. (11) the connection between ρ and p ,

$$p = 1 - 4 \int_0^{\pi/2} d\theta \cos\theta \sin^3\theta \exp(-2\rho/\cos\theta).$$

IV. SYMMETRY CLASSIFICATION OF SURFACE STATES

Equations defining a problem usually have a number of symmetries. Solutions of these equations may either have all the same symmetries or some of the symmetries may be (spontaneously) broken. The possible solutions of the problem can thus be classified according to their symmetries. In this section we present a symmetry classification of the equations discussed above in the following geometry:⁶ infinite planar wall at $x=0$ and bulk B phase in the $x \gg 0$ region and a uniform superfluid flow in the y direction in the bulk. We further assume that the solutions do not break the translational invariance in the plane of the surface (solutions with vortices are ruled out). In order to simplify the notation, the bulk B -phase order parameter $A_{\alpha i}$ is assumed to be proportional to the unit matrix. (We use the standard representation $[\Delta(\hat{\mathbf{k}})]_{\alpha} = A_{\alpha i} \hat{\mathbf{k}}_i$.) Under these assumptions, the symmetry operators very much resemble those studied by Salomaa and Volovik²¹ in the case of an isolated vortex. The operators are $P_1=R_z$, $P_2=TR_y$, and $P_3=P_1P_2$, where R_y and R_z are reflection operators in the x - z and x - y planes, respectively. In the absence of a magnetic field the time inversion operator T reduces to complex conjugation. Because two of the symmetries imply the third, there are five different symmetry classes: one having no symmetry, three having one each, and one having all the symmetries.

If there is no current there are more possible symmetries: Rotation symmetry around the x axis by an arbitrary angle (C_x) is allowed and the time-inversion symmetry can be present independent of the rest. Of these one can construct four new point symmetries: $P_4=T$, $P_5=TP_1=TR_z$, $P_6=TP_2=R_y$, and $P_7=TP_3=R_yR_z$. The last of the list is the discrete rotation symmetry around the x axis by 180° . There are now more symmetry classes than before. Five of them include the continuous rotation symmetry and they are the same as those in the presence of a current apart from the additional rotation symmetry. The classes not having the continuous rotation symmetry are as follows: There is one state having no symmetry at all, there are a number of states having one point symmetry (R_i , $i=1, \dots, 7$), there are states having two point symmetries, and so on. By this procedure one generates a great number of states, most of them equivalent however, i.e., the same except for a rotation around x . Sifting through all of them, 12 turn out to be nonequivalent. They are listed in Table I.

Knowing the symmetries of a solution, one can often simplify the corresponding equation (number of variable of the equation). For example, for the most symmetric surface state one finds the order parameter to have the form

$$A = \begin{pmatrix} R_1 & 0 & 0 \\ 0 & R_2 & 0 \\ 0 & 0 & R_2 \end{pmatrix} \quad (12)$$

in the absence of current (class 17 of Table I), and

TABLE I. The 17 symmetry classes for surface textures in case there is no current in the bulk. One possible set of symmetry operations is shown for each class (different sets for each class can be generated by rotating the symmetry operations around the surface normal). As in the main text, C_x denotes rotational symmetry around x , R_i 's the reflections, and T the time inversion. In the case in which there is a superflow in the y direction, only symmetry classes 1–4 and 7 are possible.

Number of class	Symmetries
1	No symmetry
2	R_z
3	TR_y
4	TR_yR_z
5	T
6	R_yR_z
7	R_z, TR_y, TR_yR_z
8	T, R_z, TR_z
9	T, R_yR_z, TR_yR_z
10	R_y, R_z, R_yR_z
11	TR_y, TR_z, R_yR_z
12	All point symmetries
13	C_x
14	C_x, R_z
15	C_x, TR_y
16	C_x, TR_yR_z
17	C_x , all point symmetries

$$A = \begin{pmatrix} R_1 & iR_4 & 0 \\ iR_5 & R_2 & 0 \\ 0 & 0 & R_3 \end{pmatrix} \quad (13)$$

in the presence of a current (class 7). Here the R_i 's are real functions of x .

V. METHOD OF SOLUTION

Equations (1)–(3), (9), and (10) were solved self-consistently by iterating Δ and $\hat{\sigma}_{\text{imp}}$. The former iteration was carried out as in Ref. 17 (see Ref. 22 for a generalization). The crucial point in the whole procedure is the handling of the ELOE equation (1a) and it is discussed below.

The most important single property of the quasiclassical equation (1a) is that the commutator of any two of its solutions is another solution. In addition to being analytically useful, this property supplies a technique of solving the equation numerically. Assuming a spatially constant order parameter, it is easy to see that there are three different types of solution. One group is position independent; the rest are exponentially increasing or exponentially decreasing along a trajectory. Near a wall, only such solutions can be physical which either turn into constant solutions in the bulk or decrease exponentially into the bulk. Numerically, only exponentially increasing solutions along a trajectory can be found because of the instability toward the largest eigenvalue. Solutions decaying into the bulk have to be computed moving toward the surface and starting with the known analytic forms in the bulk. The constant solutions are trickier. It seems to us

that the most powerful method of getting at them is an explosion trick where one calculates an exponentially increasing and exponentially decreasing solution (backward) and then the commutator of these. If one chooses the starting solutions correctly, this procedure generates the physical constant solution.

Analysis of the ELOE equation reveals that there is a transformation from variables $g, \underline{g}, \underline{g}, f, \underline{f}, \underline{f}$, and \underline{f} of Eq. (2b) to another set $A, B, C, D, \underline{A}, \underline{B}, \underline{C}$, and \underline{D} ,

$$2A = f + \underline{f}, \quad 2B = f - \underline{f}, \quad 2\underline{A} = \underline{f} + \underline{f}, \quad 2\underline{B} = \underline{f} - \underline{f}, \quad (14)$$

$$2C = g + \underline{g}, \quad 2D = g - \underline{g}, \quad 2\underline{C} = \underline{g} + \underline{g}, \quad 2\underline{D} = \underline{g} - \underline{g},$$

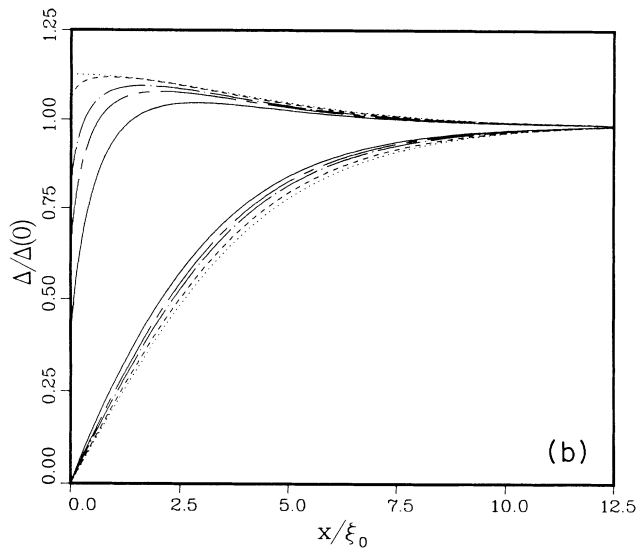
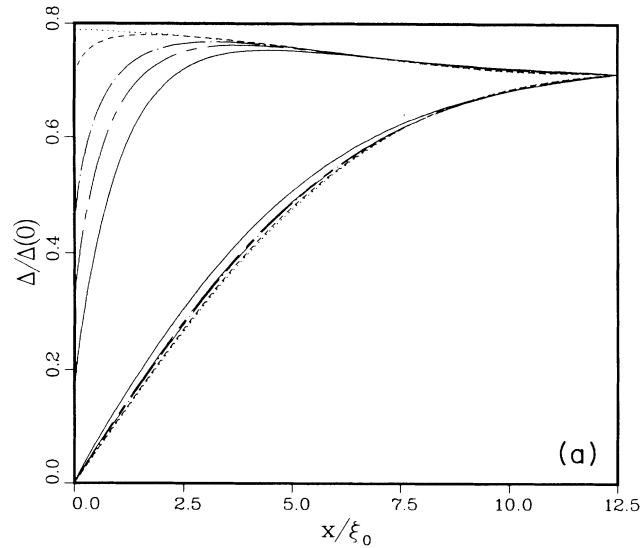


FIG. 1. Order parameter of $^3\text{He-B}$ in the vicinity of a wall. In (a) five different roughnesses are shown for $\rho=0, 0.02, 0.1, 0.2$, and 1.0 at $t=0.8$; in (b) is shown the same at $t=0.4$. The upper cluster of lines is the parallel component, the lower the perpendicular component. The roughness increases from top to bottom in the upper and bottom to top in the lower.

which separates the matrix ELOE equation into three independent sets of equations. In the present geometry (Sec. IV), they can be written as (outside of the scattering layer)

$$i\frac{\hbar v_F}{2}k_x \frac{d}{dx} C = 0, \quad (15)$$

$$i\frac{\hbar v_F}{2}k_x \frac{d}{dx} C - i\mathbf{v} \times \mathbf{C} + i\Delta_I A - \Delta_R B = 0, \quad (16a)$$

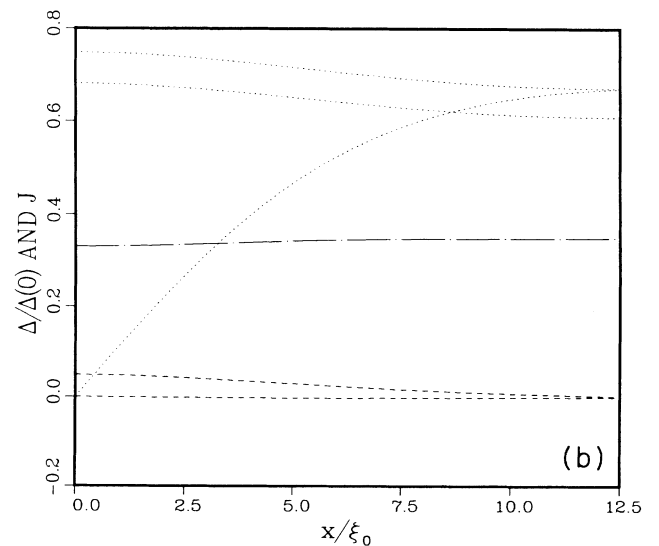
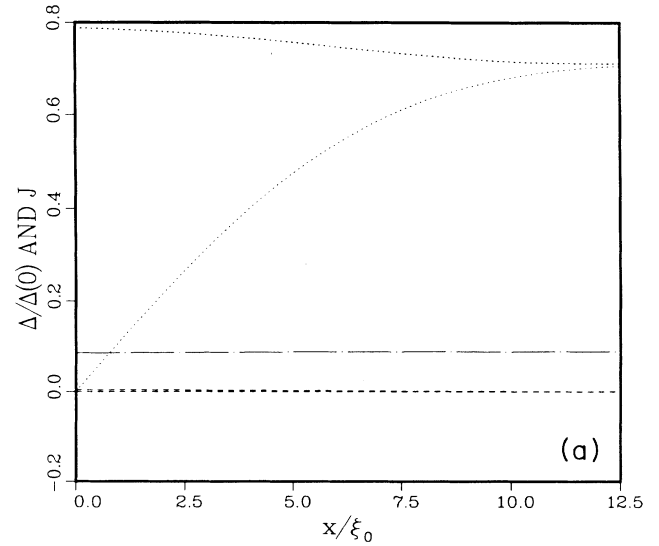


FIG. 2. Order parameter near a specularly scattering wall at $t=0.8, F_i=0$ at different phase-gradient parameters λ [Eq. (19)]. The resulting current is indicated as a dashed-dotted line in units of $N(E_F)k_B T_c v_F/2$. Dotted lines indicates the real part of the order-parameter components and dashed lines indicate the off-diagonal imaginary part of the order-parameter components. (a) and (b) are for $\lambda=0.1$ and 0.5 , respectively.

$$i\frac{\hbar v_F}{2}k_x\frac{d}{dx}A + \left[i\varepsilon_n - v - \frac{\hbar v_F}{2}qk_y\right]B + i\Delta_I \cdot C = 0, \quad (16b)$$

$$i\frac{\hbar v_F}{2}k_x\frac{d}{dx}B + \left[i\varepsilon_n - v - \frac{\hbar v_F}{2}qk_y\right]A + \Delta_R \cdot C = 0, \quad (16c)$$

$$i\frac{\hbar v_F}{2}k_x\frac{d}{dx}D + i\Delta_I \cdot A - \Delta_R \cdot B = 0, \quad (17a)$$

$$i\frac{\hbar v_F}{2}k_x\frac{d}{dx}D - i\mathbf{v} \times \mathbf{D} + i\Delta_R \times \mathbf{A} + \Delta_I \times \mathbf{B} = 0, \quad (17b)$$

$$i\frac{\hbar v_F}{2}k_x\frac{d}{dx}\mathbf{A} + \left[i\varepsilon_n - v - \frac{\hbar v_F}{2}qk_y\right]\mathbf{B} - i\mathbf{v} \times \mathbf{A} + i\Delta_I D - i\Delta_R \times \mathbf{D} = 0, \quad (17c)$$

$$i\frac{\hbar v_F}{2}k_x\frac{d}{dx}\mathbf{B} + \left[i\varepsilon_n - v - \frac{\hbar v_F}{2}qk_y\right]\mathbf{A} - i\mathbf{v} \times \mathbf{B} + \Delta_R D + \Delta_I \times \mathbf{D} = 0. \quad (17d)$$

Here,

$$\Delta(x, y, z) = \exp(iqy)[\Delta_R(x) + i\Delta_I(x)]$$

and the symmetry (6) has been applied to simplify the self-energy (but not the Green's function). The reduction to the sets (16) and (17) works in the absence of a magnetic field irrespective to the geometry. The physical solution is contained in the third set of (17). The first two sets do not satisfy the symmetry (6). (They would satisfy $\hat{g}^{\text{tr}} = +\hat{\tau}_2 \hat{g} \hat{\tau}_2$.) Nevertheless, the *second* set of Eqs. (16) (with a constant self-energy) has three constant solutions, a single exponentially increasing solution, and a single decaying one. Furthermore, the commutator of these exponentially increasing and exponentially decreasing solutions turns out to be the constant physical solution of the physical third set. This remains true in a varying order-parameter field as well. The exponentially increasing and decreasing solutions of the second block are very easy to find. They appear automatically in a numerical computation forward and backward on the trajectory with a few coherence lengths whatever the initial conditions. In this way the constant physical solution is determined as a commutator at each point of the trajectory. An apparent problem arises near a wall. There is no way of generating the purely inward (into the fluid) exploding solution at such points (because the analytic solutions are unknown)

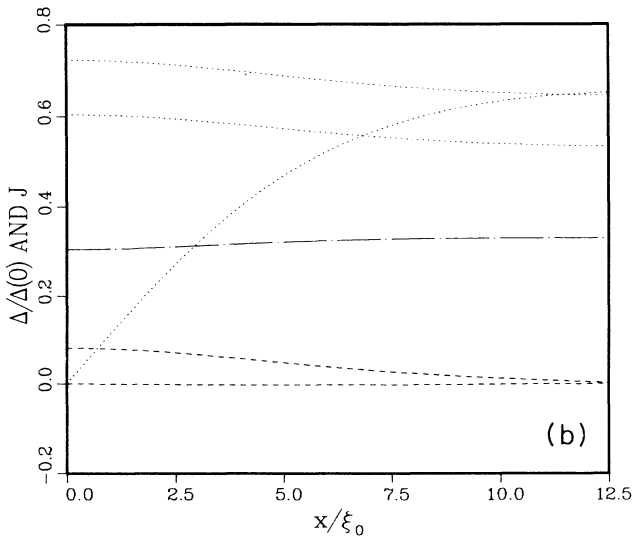
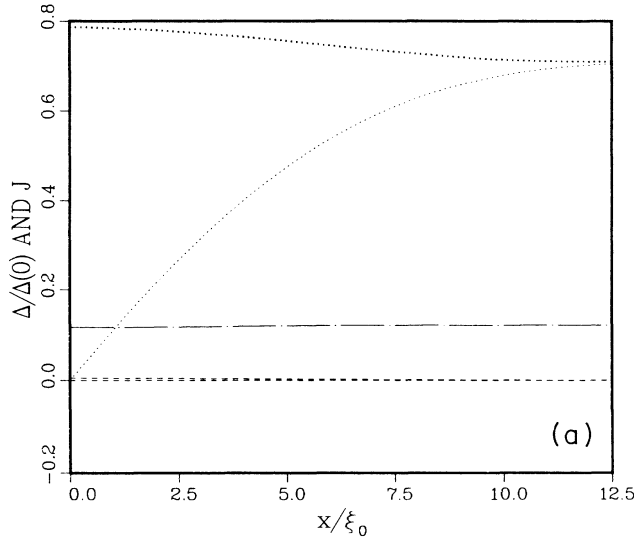


FIG. 3. Same as Fig. 2, but now at $F_1^i = 9.27$. (a) and (b) are for $\lambda = 0.1$ and 0.45 , respectively.

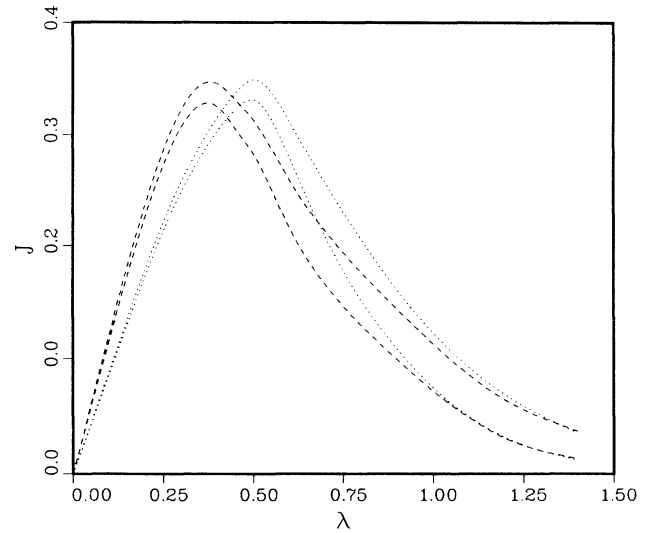


FIG. 4. Current vs phase-gradient parameter at $F_1^i = 0$ (dotted pair) and $F_1^i = 9.27$ (dashed pair). The upper curve corresponds to the bulk and lower to the wall.

and one is forced to accept a mixture for calculating the commutator with the outward (toward the wall) diverging solutions. This leads to a linear combination of the physical constant solution and inward decaying solutions. In order to meet the boundary condition, one then mixes the correct additional dose of each of the three inward decaying solutions of the third block of Eqs. (17). The result is the complete physical solution.

It would obviously be possible to limit all calculations to the physical third set of equations. There are, however, three decreasing and increasing solutions there. This would force one into a relatively complicated procedure of picking the correct constant solution among the commutators of the different pairs of exponentially varying solutions.

It may be worth mentioning here that the boundary

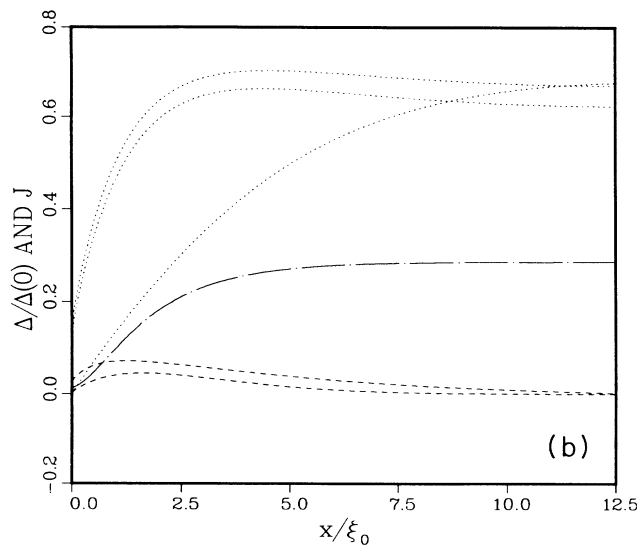
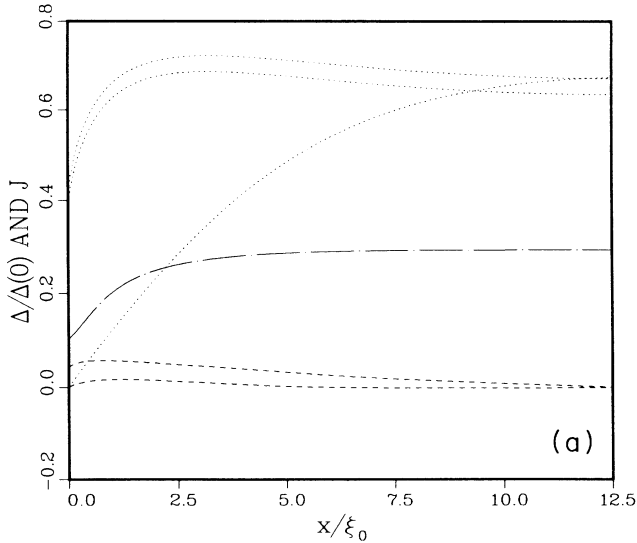


FIG. 5. Effect of the surface roughness on the order parameter with phase gradient parameter $\lambda=0.3$ at $t=0.8$ and $F_1^{\dagger}=9.27$. (a) $\rho=0.1$; (b) $\rho=1.0$. Lines as in Fig. 2.

condition is mathematically well posed. There are six complex unknowns in the third set (the amplitudes of the outward exploding solutions). The continuity of the solution at the wall gives 10 complex conditions. However, the normalization condition (1b) for the third set reads

$$D^2 + \mathbf{D}^2 - \mathbf{A}^2 + \mathbf{B}^2 = -(\pi\hbar)^2, \quad (18a)$$

$$i\mathbf{D}\mathbf{D} = \mathbf{A} \times \mathbf{B}, \quad (18b)$$

which says that four of the 10 conditions are automatically satisfied.

It is sometimes possible to reduce the number of degrees of freedom in \hat{g} by exploiting the symmetries of the order parameter (discussed in Sec. IV). All the components of \hat{g} (14) are either real or pure imaginary if the time-inversion symmetry (T) applies. The rotational symmetry (C_x) together with a reflection symmetry (for example, R_z) set four of the components in the physical set to zero. If there is current flow, however, none of the above works, and one has to keep all the 10 complex degrees of freedom in the physical set. The point symmetries (P_1 , P_2 , and P_3) can then be used only to reduce the number of momentum directions in the numerical calculation.

VI. NUMERICAL RESULTS

No symmetry restrictions were placed on the numerical search for the order parameter except for the translational symmetry along the wall. As we were looking for a phase transition on the surface, an important negative result of the study was that all the computed surface configurations belong to the same symmetry class, i.e., the most symmetric one having all the symmetries P_1, P_2, P_3 . The currentless conventional states have, in addition, the continuous rotation symmetry around the axis perpendicular to the wall. The new metastable state is an exception

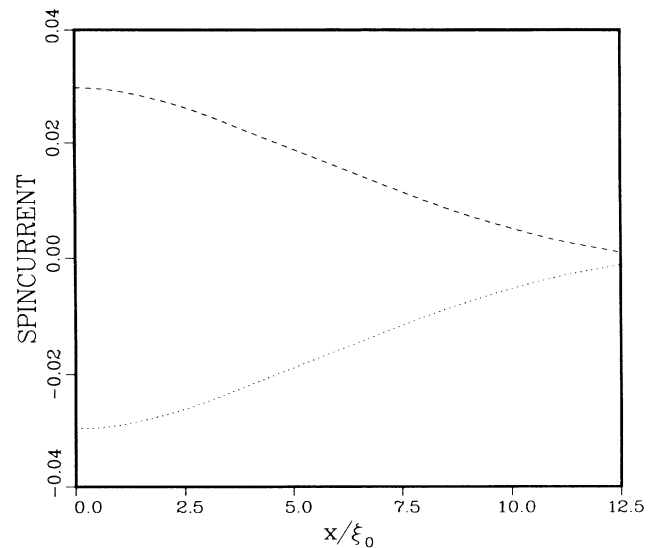


FIG. 6. Spin current in units of $N(E_F)k_B T_c \hbar v_F / 2$ at $t=0.8$, $F_1^{\dagger}=0$, $\lambda=0$, and $\rho=0$. Dotted line for J_{zx} and dashed line for J_{yz} . ($J_{zy} = -J_{yz}$) because of the symmetry requirement.)

from this rule. The results of our calculation are displayed in Figs. 1–7. Throughout, the order parameter is scaled by the bulk gap at $T=0$ and the distance from the wall by the zero-temperature coherence length $\xi_0 = \hbar v_F / 2\pi k_B T_c$. In Fig. 1 we study the dependence of the order-parameter configurations on the roughness of the wall at different temperatures without a current. The temperatures displayed in Figs. 1(a) and 1(b) are $t=0.8$ and 0.4; each panel includes the roughnesses $\rho=0, 0.02, 0.1, 0.2$, and 1.0 (another similar figure was published earlier¹⁷ at the temperature $t=0.3$; there, indicated values of ρ were in error and should be multiplied by a factor of 2). Two distinct clusters of curves are seen in each figure. The lower curves are the perpendicular component of the order parameter (Δ_{\perp}), the upper the parallel component (Δ_{\parallel}). It is well known that the perpendicular component

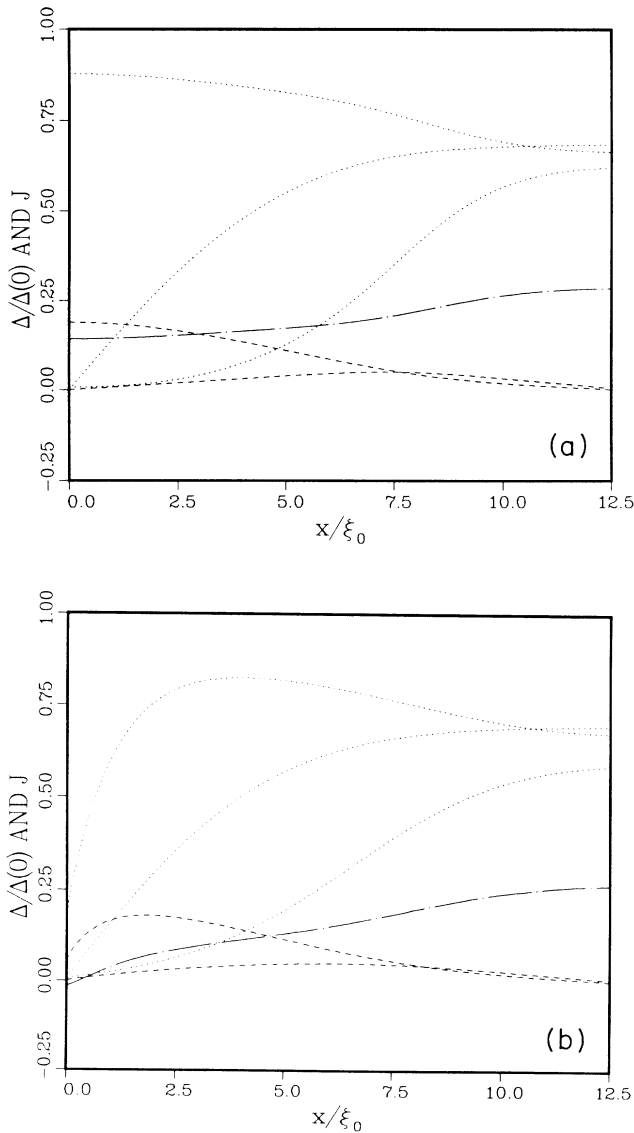


FIG. 7. The anomalous metastable state at $t=0.8$, $\lambda=0.3$, and $F_1^s=9.27$. (a) specular surface; (b) diffuse with $\rho=1.0$. Lines as in Fig. 2.

should vanish at a surface.⁵ A rough boundary is seen to kill the parallel component as well, but only a great deal closer to the wall. At a fully diffusely scattering surface, the slope of the parallel component at the wall is infinite (provided that all the Matsubara frequencies are included in the computation, see Ref. 17).

The next two sets of plots, Figs. 2 and 3, display the order parameter at a specular wall with different superfluid velocities v_s along the surface at the temperature $t=0.8$. The velocity is described by the dimensionless parameter

$$\lambda = \frac{\hbar v_F q}{2\Delta(0)} = \frac{1}{1 + F_1^s/3} \frac{p_F v_s}{\Delta(0)}. \quad (19)$$

The dashed-dotted line in the figures displays the current density, in units of $N(E_F)k_B T_c v_F/2$, near the surface. The dotted lines indicate the real part of the order-parameter components parallel and perpendicular to the wall. At higher values of λ , the parallel components are seen to split into a separate one, smaller, in the direction along the current and a larger perpendicular to the current.^{23,24} The dashed lines lowest in the figures represent the off-diagonal imaginary components iR_4 and iR_5 as seen in (13), the latter vanishing at the wall. The difference between Figs. 2 and 3 lies in the Landau parameter F_1^s which takes the value $F_1^s=9.27$ in Fig. 3 as opposed to zero in Fig. 2. It can be seen that the current is almost the same as in the bulk at all distances from the wall. This implies that the increase of Δ_{\parallel} and decrease of Δ_{\perp} near the wall almost cancel each other in the current. This is further illustrated in Fig. 4, where the current densities at the wall ($x=0$) and in the bulk ($x=\infty$) are drawn as a function of the phase gradient. It is of importance that the local maximum current is essentially independent of the position. If it were shifted to lower phase gradients near the wall, it would be indicative of an instability of the surface structure towards nucleating vortices. This would have explained why the bulk critical velocity has never been seen, but the calculation does not support such an explanation for the specular surface.

It can be seen that the most pronounced effect of the Landau parameter is slightly enhancing the current for a given phase-gradient parameter λ [but lowering for a given $p_F v_s / \Delta(0)$]. The local maximum current is almost independent of F_1^s .

Figure 5 illustrates the effect of the roughness of the surface on the order parameter in the presence of the phase-gradient parameter $\lambda=0.3$ and $F_1^s=9.27$ at $t=0.8$. The roughness reduces the order parameter essentially in the same way as seen in Fig. 1, but now the current also becomes reduced close to the surface. This is in agreement with the well-known effect that the current in superfluid for a given phase gradient is reduced (but not destroyed) by scattering.

Figure 6 shows the spin current, in units of $N(E_F)k_B T_c \hbar v_F/2$, without mass current and roughness at $F_1^s=0$ and $t=0.8$. In the presence of a current there is also a small magnetization near the wall long the z axis. More generally, if the B -phase order parameter has the form $A_{\mu j} = R_{\mu j}$ ($R_{\mu j}$ is a rotation matrix) in the bulk, the

magnetization is in the direction of $R_{\mu z}$.

We finally return to the metastable state mentioned in the Introduction. Its symmetry class is number 7 of Table I in general and number 12 in the currentless case. This state seems to persist no matter what the current or the scattering properties of the wall. In Figs. 7(a) and 7(b) we display the state for a specular surface and rough surface in the presence of a phase-gradient parameter $\lambda=0.3$. The distinguishing feature of the metastable state is the vanishing of the real part of the order-parameter component parallel to the current. It can be seen in the figures that the new vanishing component recovers quite slowly into the fluid. The current density as a function of the distance from the walls is very sensitive to the scattering properties of the surface and it is always smaller than that in the "regular" state. The magnetization in this state is much smaller than the "regular" state. We have not investigated the energy of the metastable state.

VII. CONCLUSIONS

We have investigated the order-parameter configuration

of $^3\text{He-B}$ near surfaces in the absence, as well as in the presence, of a current. Both the specular wall and the diffusely quasiparticle scattering wall were studied. Part of the motivation of the work was a search for surface phase transitions at temperatures below the strict range of validity of the Ginzburg-Landau theory. We found, however, only states of the single symmetry class including a metastable state belonging to the same symmetry class as the "regular" surface state. In the metastable state, the real part of the order-parameter component parallel to the current vanishes at the wall. We have investigated the effects of superfluid flow and surface roughness on the surface state. We did not find any sign of instability of the surface structure towards nucleating vortices below the critical velocity of the bulk, but this possibility is far from excluded by the present work. Knowing the surface structure allows the determination of the boundary conditions to impose on the superfluid (\hat{n} -vector field of $^3\text{He-B}$) and the quasiparticle degrees of freedom.²⁵

-
- ¹H. E. Hall and J. R. Hook, in *Progress in Low Temperature Physics*, edited by D. F. Brewer (North-Holland, Amsterdam, 1986), Vol. IX, p. 143.
- ²H. H. Jensen, H. Smith, P. Wölfle, K. Nagai, and T. M. Bisgaard, *J. Low Temp. Phys.* **41**, 473 (1980).
- ³D. Einzel, P. Wölfle, H. H. Jensen, and H. Smith, *Phys. Rev. Lett.* **52**, 1705 (1984).
- ⁴H. Smith, W. F. Brinkman, and S. Engelsberg, *Phys. Rev. B* **15**, 199 (1977).
- ⁵V. Ambegaokar, P. G. de Gennes, and D. Rainer, *Phys. Rev. A* **9**, 2676 (1974); **12**, 345 (1975).
- ⁶E. V. Thuneberg, *Phys. Rev. B* **33**, 5124 (1986).
- ⁷Ren-zhi Ling, D. S. Betts, and D. F. Brewer, *Phys. Rev. Lett.* **53**, 930 (1984).
- ⁸J. P. Pekola and J. T. Simola, *J. Low Temp. Phys.* **58**, 555 (1985).
- ⁹P. L. Gammel, T.-L. Ho, and J. D. Reppy, *Phys. Rev. Lett.* **55**, 2708 (1985).
- ¹⁰C. A. M. Castelijns, K. F. Coates, A. M. Guenault, S. G. Mussett, and G. R. Pickett, *Phys. Rev. Lett.* **56**, 69 (1986).
- ¹¹J. W. Serene and D. Rainer, *Phys. Rep.* **101**, 221 (1983).
- ¹²F. J. Culetto, G. Kiselmann and D. Rainer, in *Proceedings of the 17th International Conference on Low Temperature Physics—LT-17*, edited by U. Eckern, A. Schmid, W. Weber, and H. Wühl (North-Holland, Amsterdam, 1984), p. 1027.
- ¹³L. J. Buchholtz and G. Zwirnagl, *Phys. Rev. B* **23**, 5788 (1981).
- ¹⁴L. J. Buchholtz, *Phys. Rev. B* **33**, 1579 (1986).
- ¹⁵J. C. Wheatley, *Rev. Mod. Phys.* **47**, 415 (1975).
- ¹⁶E. V. Thuneberg, *Europhys. Lett.* (to be published).
- ¹⁷Weiyi Zhang, J. Kurkijärvi, and E. V. Thuneberg, *Phys. Lett.* **109A**, 238 (1985).
- ¹⁸J. A. Sauls, D. L. Stein, and J. W. Serene, *Phys. Rev. D* **25**, 967 (1982).
- ¹⁹L. J. Buchholtz and D. Rainer, *Z. Phys. B* **35**, 151 (1979).
- ²⁰G. Lüders and K. D. Usadel, in *The Method of the Correlation Function in Superconductivity Theory*, No. 56 of *Springer Tracts in Modern Physics*, edited by G. Höhler (Springer, Berlin, 1971), p. 133, Eq. (15.42).
- ²¹M. M. Salomaa and G. E. Volovik, *Phys. Rev. Lett.* **51**, 2040 (1983).
- ²²N. Schopohl and E. V. Thuneberg (unpublished).
- ²³D. Vollhardt, K. Maki, and N. Schopohl, *J. Low Temp. Phys.* **39**, 79 (1980).
- ²⁴H. Kleinert, *J. Low Temp. Phys.* **39**, 451 (1980).
- ²⁵Weiyi Zhang, J. Kurkijärvi, D. Rainer, and E. V. Thuneberg (unpublished).